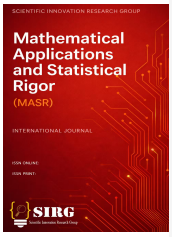

Mathematical Applications and Statistical Rigor
MASR

Journal Homepage
https://pub.scientificirg.com/index.php/MASR/index

Bi-OSW-MF-DFA: An Enhanced Multifractal Method for Gold and Silver Market Risk Assessment [1]

Zhongjun Wang[a], **Mengye Sun**[a] **and A.M. Elsawah**[b,c,d] [2]

[a] *Department of Statistics, Science School, Wuhan University of Technology, Wuhan 430070, China*
[b] *Department of Statistics and Data Science, Faculty of Science and Technology, Beijing Normal-Hong Kong Baptist University, Zhuhai 519087, China*
[c] *Guangdong Provincial/Zhuhai Key Laboratory of Interdisciplinary Research and Application for Data Science, BNBU Zhuhai 519085, China*
[d] *Department of Mathematics, Faculty of Science, Zagazig University, Zagazig 44519, Egypt*

ABSTRACT

Amid global economic uncertainty and inflationary pressures, precious metals have gained prominence as safe-haven assets, yet accurately quantifying their risk remains challenging due to the inherent limitations of existing fractal analysis methods. Conventional Multifractal Detrended Fluctuation Analysis (MF-DFA) suffers from boundary-induced artifacts and computational inefficiencies, which can distort risk measurements and obscure true market dynamics. To address this gap, we introduce an enhanced method—Binary Overlapped Sliding Window MF-DFA (Bi-OSW-MF-DFA)—that mitigates segmentation discontinuities and improves computational robustness through overlapping windows and binary series partitioning. Applied to spot gold and silver markets, our approach reveals that silver exhibits stronger multifractality and higher inherent risk than gold, with long-range temporal correlations identified as the primary driver of multifractal behavior. This study offers a refined analytical framework for market risk assessment and provides actionable insights for investors and portfolio managers navigating precious metals volatility.

PAPER INFORMATION

HISTORY
Received: 10 September 2025
Revised: 2 December 2025
Accepted: 12 January 2026
Online: 26 January 2026

MSC
62M10
62P20
91G70

KEYWORDS
MF-DFA
Fractal theory
Risk assessment
Bi-OSW-MF-DFA
Multifractal analysis
Precious metals market

1 Introduction

The rapid expansion of global capital markets has witnessed a proliferation of financial instruments, with precious metals emerging as a significant component within diversified investment portfolios. Gold and silver, as primary assets in this sector, attract substantial attention due to their pronounced price volatility and their traditional role as safe-haven investments during periods of economic uncertainty and financial crisis. However, financial markets constitute complex adaptive systems shaped by a multitude of interconnected factors, rendering their precise characterization a persistent challenge [1].

Extant research reveals that price dynamics in precious metals markets exhibit pronounced non-linear characteristics and complex multifractal properties. For instance, empirical studies demonstrate distinct

[1] A preprint version of this paper is available on arXiv at `https://arxiv.org/abs/2006.15214`
[2] Corresponding author at Beijing Normal-Hong Kong Baptist University, China. E-mail: amelsawah@ybnbu.edu.cn.

multifractal signatures in gold price indices across emerging economies such as China, India, and Turkey [2]. Investigating multifractality in financial time series provides critical insights into market microstructure, offering valuable information on market efficiency, persistence, and underlying risk factors [3].

Fractal theory, pioneered by Mandelbrot [4], provides a powerful analytical framework for characterizing complex systems with self-similar properties. Its application to finance has offered novel perspectives beyond traditional linear models. The rescaled range analysis (R/S), introduced by Hurst [5], was an early method for detecting long-term dependence. Subsequent methodological refinements, such as the q-th order height-height correlation function, extended R/S analysis to multifractal contexts, as evidenced in studies of the Korean stock market [6].

While conventional R/S analysis and detrended fluctuation analysis (DFA) are effective for characterizing monofractal processes [7, 8, 9], they are inadequate for capturing the intricate dynamics governed by multiple scaling exponents [10]. To address this, [11] introduced Multifractal Detrended Fluctuation Analysis (MF-DFA), which has become a standard methodology for investigating long-range correlations in non-stationary time series while mitigating spurious correlation artifacts. The MF-DFA framework has been widely applied to financial markets, yielding significant insights into market efficiency, volatility clustering, and risk transmission mechanisms [12, 13, 14, 15].

Empirical applications of MF-DFA continue to reveal important market characteristics. [16] demonstrated that degrees of multifractality correlate with stages of market development across international equity markets. [17] employed MF-DFA to quantify multifractality in stock index fluctuations, while [18] investigated the compositional sources of empirical multifractality in financial returns. Despite its widespread adoption, the conventional MF-DFA methodology is not without limitations. A notable drawback is the potential for boundary discontinuities arising from independent polynomial fitting in adjacent, non-overlapping segments, which can introduce artifacts and distort the estimation of scaling behavior [19].

This study makes two primary contributions to the literature. First, we develop an enhanced MF-DFA methodology—Binary Overlapped Sliding Window-based MF-DFA (Bi-OSW-MF-DFA)—that directly addresses the boundary discontinuity problem and improves computational efficiency. Second, we apply this refined framework to conduct a comprehensive comparative analysis of the multifractal properties and associated risk profiles in spot gold and silver markets. Our investigation provides novel insights into the structural determinants of multifractality in precious metals and their practical implications for risk management and investment strategy.

The remainder of this paper is structured as follows. Section 2 details the theoretical foundations of MF-DFA and presents our methodological innovations. Section 3 applies the Bi-OSW-MF-DFA framework to empirical data from gold and silver markets, including a comparative risk assessment. Section 4 synthesizes the findings, discusses their implications, and suggests directions for future research.

2 Methodology: Improving the MF-DFA Framework

2.1 Review of MF-DFA Methodology

Multifractal Detrended Fluctuation Analysis (MF-DFA) has been widely applied across various scientific disciplines to reliably determine the multifractal scaling behavior of non-stationary time series [11]. The method consists of six sequential steps, which we outline below.

Step 1: Profile Construction: Given a time series $\{x_k\}$ of length N, we first compute its cumulative deviation from the mean, known as the "profile":

$$Y(i) = \sum_{k=1}^{i} (x_k - \bar{x}), \quad i = 1, 2, \ldots, N, \quad \bar{x} = \frac{1}{N} \sum_{i=1}^{N} x_i. \tag{1}$$

Step 2: Segmentation: The profile $Y(i)$ is divided into $N_s = \lfloor N/s \rfloor$ non-overlapping segments of equal length s, where $\lfloor \cdot \rfloor$ denotes the floor function. Since N may not be an exact multiple of s, a residual portion at the end of the profile is often disregarded. To preserve data integrity, the procedure is repeated starting from the opposite end of the series, yielding a total of $2N_s$ segments.

Step 3: Local Detrending and Variance Calculation: For each of the $2N_s$ segments, a local polynomial trend $y_v(i)$ is estimated via least-squares regression. The variance around this trend is then computed.

For the first N_s segments ($v = 1, \ldots, N_s$):

$$F^2(v,s) = \frac{1}{s}\sum_{j=1}^{s}\left(Y((v-1)s+j) - y_v(j)\right)^2. \tag{2}$$

For the remaining segments obtained from the reverse traversal ($v = N_s+1, \ldots, 2N_s$):

$$F^2(v,s) = \frac{1}{s}\sum_{j=1}^{s}\left(Y(N-(v-N_s)s+j) - y_v(j)\right)^2. \tag{3}$$

The order of the detrending polynomial (m) can be adjusted; common choices are linear ($m = 1$; MF-DFA1), quadratic ($m = 2$; MF-DFA2), or cubic ($m = 3$; MF-DFA3).

Step 4: Fluctuation Function Computation: The qth-order fluctuation function $F_q(s)$ is obtained by averaging over all segments:

$$F_q(s) = \left(\frac{1}{2N_s}\sum_{v=1}^{2N_s}\left[F^2(v,s)\right]^{q/2}\right)^{1/q}, \quad q \in \mathbb{R}\setminus\{0\}. \tag{4}$$

For the special case $q = 0$, the logarithmic averaging is applied:

$$F_0(s) = \exp\left(\frac{1}{2N_s}\sum_{v=1}^{2N_s}\ln\left[F^2(v,s)\right]\right). \tag{5}$$

Step 5: Scaling Analysis and Generalized Hurst Exponent: The scaling behavior is examined by plotting $\log F_q(s)$ against $\log s$. If long-range power-law correlations exist, then:

$$F_q(s) \sim s^{h(q)}, \tag{6}$$

where $h(q)$ is the generalized Hurst exponent. For $q = 2$, $h(2)$ corresponds to the classical Hurst exponent H. A monofractal series exhibits $h(q)$ independent of q, while for multifractal series, $h(q)$ varies with q. The degree of multifractality is quantified by:

$$\Delta h = h(q_{\min}) - h(q_{\max}) > 0. \tag{7}$$

For $h(q) > 0.5$, fluctuations exhibit persistent auto-correlation; for $h(q) < 0.5$, anti-persistent correlation; and $h(q) = 0.5$ indicates random walk behavior [3].

Step 6: Multifractal Spectrum Analysis: The multifractal scaling exponent $\tau(q)$ and singularity spectrum $f(\alpha)$ provide complementary characterizations:

$$\tau(q) = qh(q) - 1. \tag{8}$$

A linear $\tau(q)$ versus q relationship indicates monofractality, while nonlinearity signifies multifractality. The singularity strength α and spectrum $f(\alpha)$ are derived via Legendre transform:

$$\alpha(q) = \frac{d\tau(q)}{dq} = h(q) + qh'(q), \tag{9}$$

$$f(\alpha) = q\alpha(q) - \tau(q) = q^2h'(q) + 1. \tag{10}$$

The width of the singularity spectrum, $\Delta\alpha = \alpha_{\max} - \alpha_{\min}$, measures the heterogeneity in the fractal structure; wider $\Delta\alpha$ indicates stronger multifractality and typically greater market risk [13, 19, 20].

2.2 Improving MF-DFA Methodology: Bi-OSW-MF-DFA

We propose two key modifications to the standard MF-DFA procedure to enhance its robustness and computational efficiency, naming the improved method Binary Overlapped Sliding Window-based MF-DFA (Bi-OSW-MF-DFA).

Modification 1: Binary Partitioning: Rather than processing the entire profile at once, we first partition $Y(i)$ into two approximately equal sub-series:

$$n = \left\lfloor \frac{N}{2} \right\rfloor. \tag{11}$$

This yields two sub-series: $Y_1(i)$ for $i = 1, \ldots, n$ and $Y_2(i)$ for $i = n+1, \ldots, N$. If N is odd, Y_2 contains one additional observation.

Modification 2: Overlapped Sliding Windows: Each sub-series is then divided using overlapping segments. For a given segment length s and overlap length l ($0 < l < s/2$), the number of segments in one direction for a sub-series of length n is:

$$N_s^* = \left\lfloor \frac{n-s}{s-l} \right\rfloor + 1. \tag{12}$$

To utilize all data and maintain consistency with the standard MF-DFA approach, we repeat this segmentation starting from the opposite end of each sub-series. This yields $2N_s^*$ segments per sub-series, resulting in a total of $4N_s^*$ segments across both sub-series.

Visual Comparison of Segmentation Strategies The segmentation strategies of standard MF-DFA and the proposed Bi-OSW-MF-DFA are visually compared in Figure 1. Panel (a) illustrates the standard MF-DFA approach with sequential non-overlapping segmentation. Panel (b) shows the reverse segmentation used to include residual data. Panel (c) demonstrates our proposed Bi-OSW-MF-DFA method, where the series is first partitioned into two sub-series (binary partitioning), and then overlapping windows are applied to each sub-series. This visual representation clarifies how our method reduces boundary discontinuities through overlapping windows while maintaining data coverage through binary partitioning.

2.3 Advantages of the Bi-OSW-MF-DFA Method

The Bi-OSW-MF-DFA method offers two principal advantages over conventional MF-DFA.

First, it mitigates boundary artifacts. A known limitation of standard MF-DFA is that independent polynomial fitting in adjacent, non-overlapping segments can cause abrupt jumps in the detrended profile at segment boundaries [16]. By employing overlapping windows, our method ensures smoother transitions between segments, leading to more stable fluctuation estimates.

Second, it improves statistical efficiency. The use of overlapping windows increases the effective number of segments, reducing the variance of the fluctuation function estimates. While standard MF-DFA yields $2N_s$ segments, Bi-OSW-MF-DFA produces $4N_s^*$ segments, typically resulting in $N_s^* > N_s$ for reasonable overlap choices.

The fluctuation function in Bi-OSW-MF-DFA is computed as:

$$F_q(s) = \left(\frac{1}{4N_s^*} \sum_{v=1}^{4N_s^*} \left[F^2(v,s) \right]^{q/2} \right)^{1/q}, \tag{13}$$

with appropriate adjustment for $q = 0$ following Equation (5). As we demonstrate empirically in Section 3, this formulation yields more robust and concentrated estimates of $h(q)$, confirming the enhanced performance of our proposed method.

3 Empirical Analysis for Risk Assessment of Gold and Silver Markets

3.1 Data Description and Preliminary Analysis

This study investigates the multifractal characteristics of precious metals markets using daily closing prices of spot gold (February 9, 2004 to March 23, 2015) and spot silver (February 13, 2004 to March 23, 2015). After removing weekends and holidays, we obtain 2,851 observations for gold and 2,880 for silver. All data are sourced from the JIJIN silver and gold analysis software. Figure 2 presents the price trajectories for both metals.

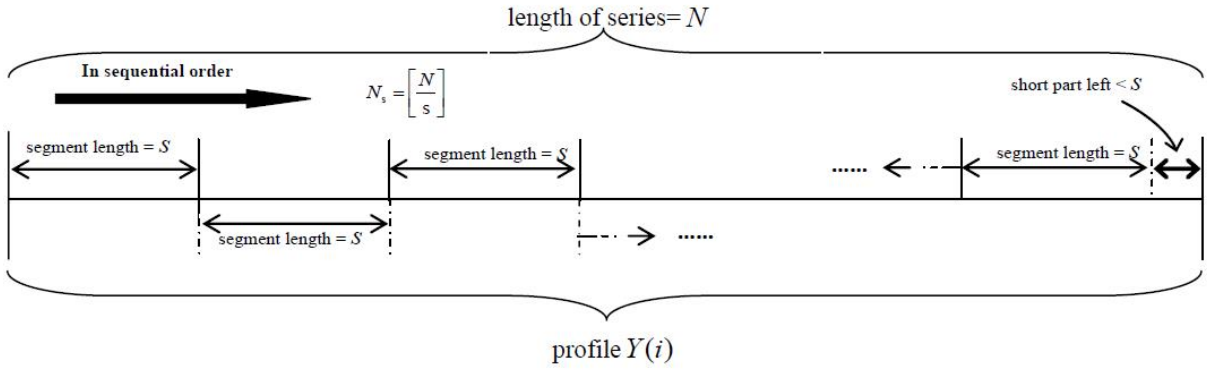

(a) MF-DFA: sequential segmentation

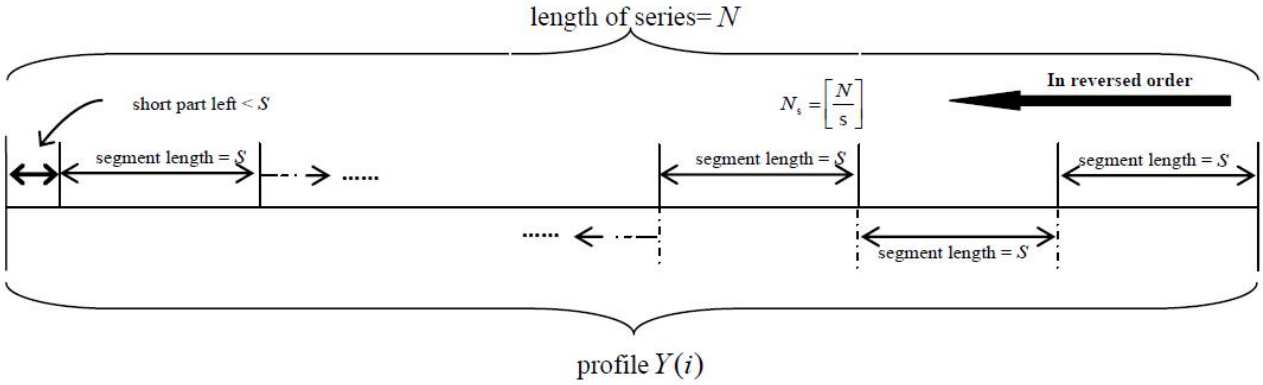

(b) MF-DFA: reverse segmentation

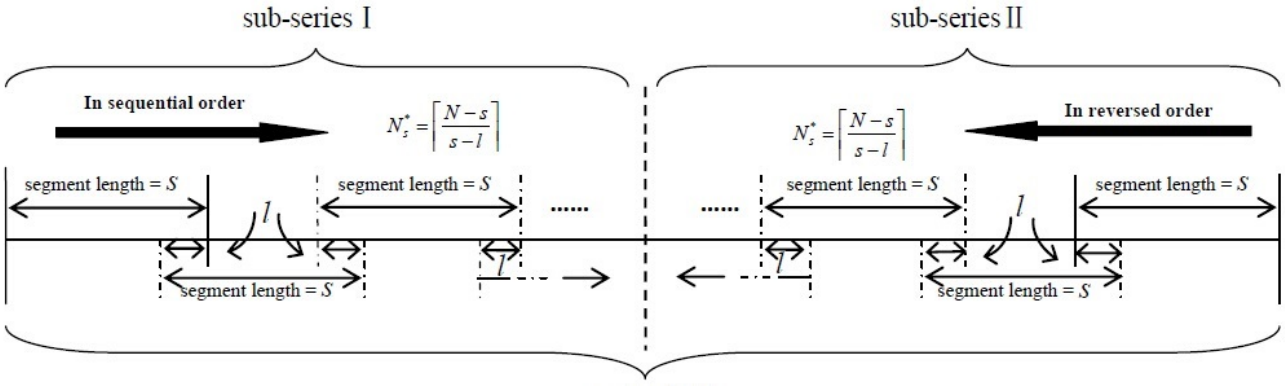

(c) Bi-OSW-MF-DFA: overlapping segmentation

Figure 1: Comparison of segmentation strategies in MF-DFA and Bi-OSW-MF-DFA methods. (a) Standard MF-DFA with sequential segmentation. (b) Standard MF-DFA with reverse segmentation to include residual data. (c) Proposed Bi-OSW-MF-DFA with overlapping windows on partitioned series.

We first test the stationarity of both price series using the Augmented Dickey-Fuller (ADF) test, which examines the presence of unit roots [21]. Tables 1 and 2 present the ADF test results for gold and silver, respectively. The test specification includes a constant term but no trend, denoted as $(c, 0, p)$, where p is the lag order determined by the Schwarz Information Criterion.

Both series are non-stationary in levels but stationary in first differences. To eliminate the dependence of price fluctuations on price levels, we compute logarithmic returns:

$$r_t = \ln(I_t) - \ln(I_{t-1}), \tag{14}$$

where I_t denotes the closing price at time t. This transformation yields 2,850 and 2,879 daily return observations for gold and silver, respectively. The return series are visualized in Figure 3.

Table 3 presents descriptive statistics for the return series. Both exhibit negative skewness and excess kurtosis greater than 3, indicating departure from normality and the presence of fat-tailed distributions, which is consistent with typical financial return series and suggests the need for multifractal analysis.

Table 1: ADF test results for spot gold daily closing price series.

Variable	(c, t, p)	ADF Statistic	1% Critical	5% Critical	10% Critical	p-value	Conclusion
Y	$(c, 0, 0)$	1.378	-2.568	-1.941	-1.617	0.958	Nonstationary
ΔY	$(c, 0, 1)$	-30.135	-2.568	-1.941	-1.617	0.000	Stationary

Table 2: ADF test results for spot silver daily closing price series.

Variable	(c, t, p)	ADF Statistic	1% Critical	5% Critical	10% Critical	p-value	Conclusion
Y	$(c, 0, 0)$	0.571	-2.568	-1.941	-1.616	0.839	Nonstationary
ΔY	$(c, 0, 1)$	-32.178	-2.568	-1.941	-1.616	0.000	Stationary

Table 3: Descriptive statistics of daily return series.

Series	N	Mean	Minimum	Maximum	Skewness	Kurtosis
Gold	2,879	0.0003	-0.20	0.13	-1.074	8.358
Silver	2,850	0.0004	-0.11	0.10	-0.416	6.706

3.2 Methodological Comparison: MF-DFA vs. Bi-OSW-MF-DFA

Precious metals markets constitute complex nonlinear dynamic systems with asymmetric information flows, making price fluctuations challenging to predict [2]. To assess the scaling properties of these markets, we examine the fluctuation functions $F_q(s)$ obtained via both standard MF-DFA and our proposed Bi-OSW-MF-DFA method. Figures 4a and 4b display $F_q(s)$ versus scale s for selected q values (-20, -10, -2, 2, 10, 20) using Bi-OSW-MF-DFA.

The presence of crossover points in the log-log plots indicates multiple scaling regimes, necessitating multifractal analysis [11]. To validate the robustness of our improved method, we compare the generalized Hurst exponents $h(q)$ obtained from both methods for identical parameter settings (time scales s from 10 to 50, detrending polynomial order $m = 2$).

Table 4 presents $h(q)$ values for both metals using both methods. The degree of multifractality, measured by $\Delta h = h(q_{\min}) - h(q_{\max})$, is consistently smaller for Bi-OSW-MF-DFA: $\Delta h_g^* = 0.3860 < \Delta h_g = 0.5965$ for gold, and $\Delta h_s^* = 0.5515 < \Delta h_s = 0.8501$ for silver. This reduction in Δh indicates that Bi-OSW-MF-DFA produces more concentrated and stable estimates of $h(q)$, confirming its superior robustness.

The dependence of $h(q)$ on q, visualized in Figures 5a and 5b, confirms multifractality in both markets. Silver exhibits stronger multifractality ($\Delta h_s^* = 0.5515$) than gold ($\Delta h_g^* = 0.3860$), suggesting higher market complexity and risk in the silver market. This finding aligns with silver's known higher volatility and speculative nature compared to gold's more stable safe-haven characteristics.

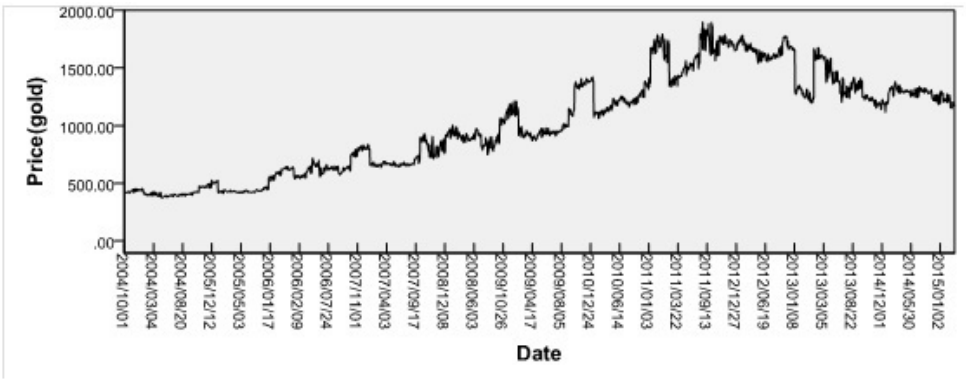

(a) Spot gold daily closing prices (2004-2015)

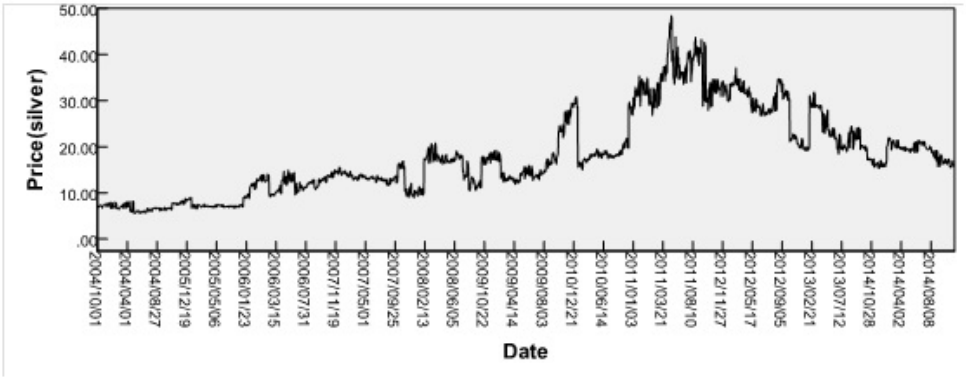

(b) Spot silver daily closing prices (2004-2015)

Figure 2: Daily closing price history of spot gold and silver markets (2004-2015).

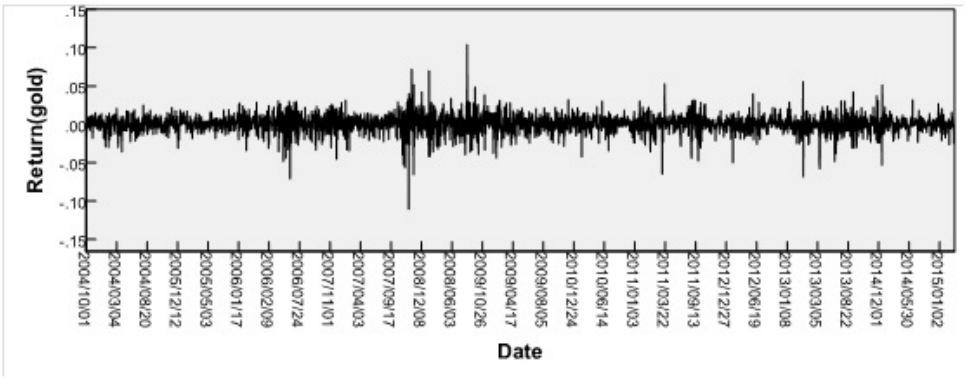

(a) Spot gold daily returns (2004-2015)

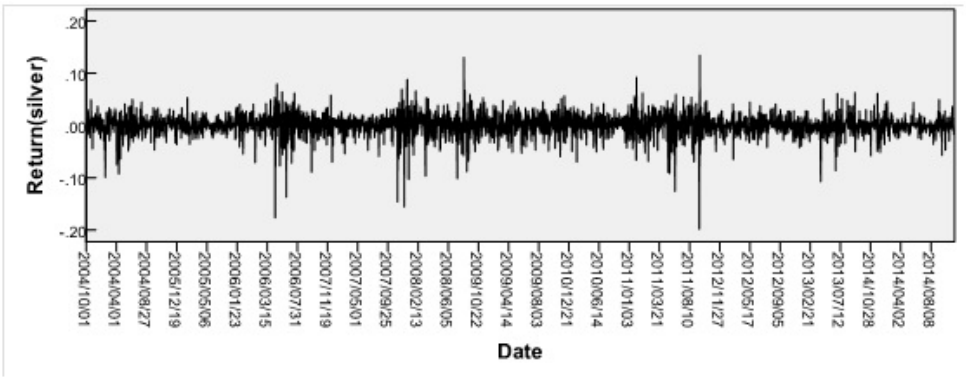

(b) Spot silver daily returns (2004-2015)

Figure 3: Daily return series of spot gold and silver markets (2004-2015).

Table 4: Generalized Hurst exponents $h(q)$ calculated via MF-DFA and Bi-OSW-MF-DFA.

q	MF-DFA		Bi-OSW-MF-DFA	
	Gold $h_g(q)$	Silver $h_s(q)$	Gold $h_g^*(q)$	Silver $h_s^*(q)$
-20	0.8704	1.0400	0.7217	0.7849
-16	0.8569	1.0237	0.7129	0.7757
-12	0.8331	0.9942	0.7005	0.7619
-8	0.7832	0.9287	0.6807	0.7398
-4	0.6887	0.7729	0.6387	0.6856
0	0.5908	0.6207	0.5546	0.5806
2	0.5316	0.5480	0.5129	0.5160
4	0.4634	0.4326	0.4719	0.4302
8	0.3629	0.2833	0.4034	0.3221
12	0.3139	0.2294	0.3674	0.2748
16	0.2885	0.2042	0.3477	0.2492
20	0.2739	0.1899	0.3357	0.2334
Δh	0.5965	0.8501	0.3860	0.5515

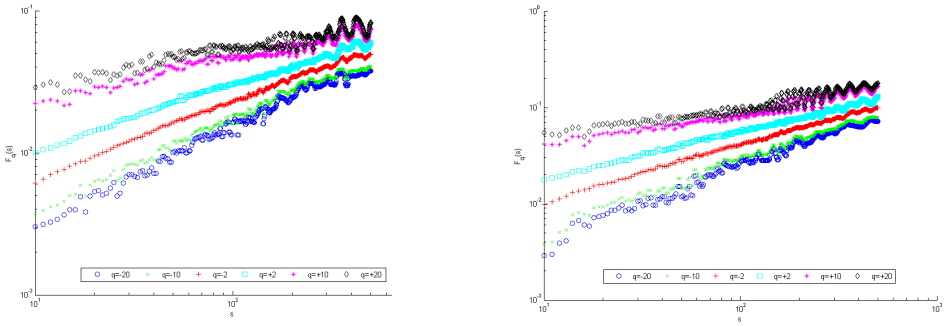

(a) Gold return series (b) Silver return series

Figure 4: Fluctuation functions $F_q(s)$ obtained via Bi-OSW-MF-DFA for selected q values. The crossover points in the log-log plots indicate multiple scaling regimes, confirming the multifractal nature of both markets.

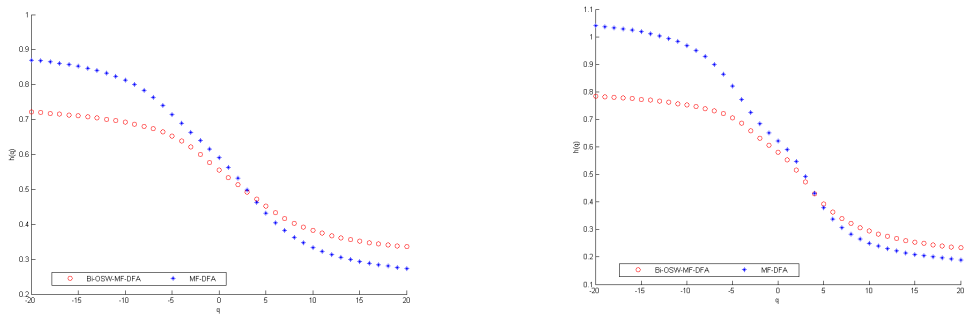

(a) Gold return series (b) Silver return series

Figure 5: Generalized Hurst exponents $h(q)$ versus order q: MF-DFA (dashed lines) vs. Bi-OSW-MF-DFA (solid lines). The dependence of $h(q)$ on q confirms multifractality, with silver showing stronger variation than gold.

3.3 Sources of Multifractality

Multifractality in financial time series typically arises from two sources: (i) broad probability density functions and (ii) different long-range correlations for small versus large fluctuations [10]. To disentangle these effects, we apply shuffling and phase randomization procedures.

Shuffling Procedure:

1. Generate random integer pairs (m, n) with $m, n \leq N$, where N is the series length.
2. Interchange entries at positions m and n.
3. Repeat steps 1–2 for $20N$ iterations to ensure complete randomization.

Phase Randomization Procedure:

1. Apply discrete Fourier transform to the original series.
2. Rotate the phase by a random angle while preserving amplitude.
3. Apply inverse Fourier transform to obtain the surrogate series.

Shuffling destroys temporal correlations while preserving the distribution, whereas phase randomization preserves linear correlations but Gaussianizes the distribution. Table 5 and Figures 6a and 6b present $h(q)$ for original, shuffled, and surrogate series.

The sharp decrease in $h(q)$ after shuffling indicates that temporal correlations dominate multifractality in both markets. The greater deviation from 0.5 for gold suggests stronger anti-persistence in gold returns. The smaller Δh for surrogate series (gold: 0.1267; silver: 0.1604) compared to shuffled series indicates that fat-tailed distributions also contribute to multifractality, particularly for silver. This decomposition reveals that approximately 67% of gold's multifractality and 73% of silver's multifractality can be attributed to long-range correlations, with the remainder stemming from distributional properties.

Table 5: Generalized Hurst exponents $h(q)$ for original, shuffled, and surrogate series.

q	Gold Return Series			Silver Return Series		
	Original	Shuffled	Surrogate	Original	Shuffled	Surrogate
-20	0.7217	0.3489	0.5862	0.7849	0.3818	0.5848
-16	0.7129	0.3144	0.5743	0.7757	0.3526	0.5766
-12	0.7005	0.2619	0.5577	0.7619	0.3052	0.5667
-8	0.6807	0.1887	0.5379	0.7398	0.2289	0.5546
-4	0.6387	0.1147	0.5243	0.6856	0.1322	0.5385
0	0.5546	0.0672	0.5195	0.5806	0.0708	0.5205
2	0.5129	0.0514	0.5176	0.5160	0.0512	0.5121
4	0.4719	0.0386	0.5142	0.4302	0.0349	0.5040
8	0.4034	0.0190	0.5015	0.3221	0.0076	0.4853
12	0.3674	0.0044	0.4852	0.2748	-0.0167	0.4611
16	0.3477	-0.0068	0.4706	0.2492	-0.0397	0.4395
20	0.3357	-0.0156	0.4595	0.2334	-0.0605	0.4244
Δh	0.3860	0.3645	0.1267	0.5515	0.4423	0.1604

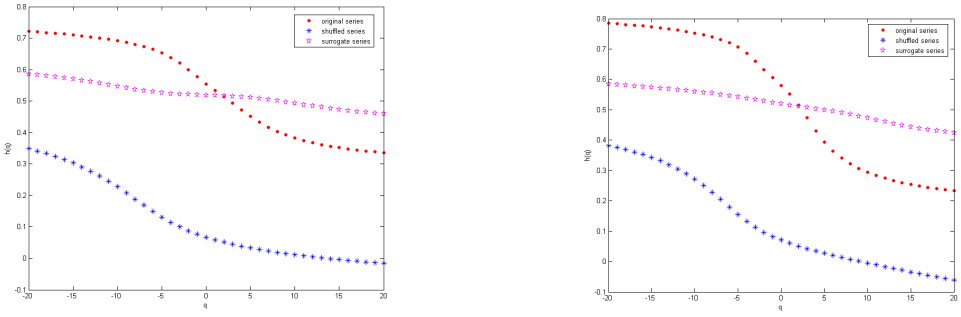

(a) Gold market (b) Silver market

Figure 6: Generalized Hurst exponents $h(q)$ for original, shuffled, and surrogate series. The sharp decline in $h(q)$ after shuffling highlights the dominant role of temporal correlations in generating multifractality.

3.4 Scaling Exponent Analysis

The multifractal scaling exponent $\tau(q) = qh(q) - 1$ provides further insight into market dynamics. For monofractal series, $\tau(q)$ is linear in q; nonlinearity indicates multifractality. Figures 7a and 7b display $\tau(q)$ versus q for original, shuffled, and surrogate series.

The pronounced nonlinearity in the original series and the shuffled series highlights the contribution of correlation structures to multifractality. Silver exhibits stronger nonlinearity than gold, indicating greater sensitivity to extreme fluctuations and higher susceptibility to sudden price movements. The near-linear behavior of the surrogate series confirms that Gaussianizing the distribution reduces but does not eliminate multifractality, supporting the finding that both correlations and distributional properties contribute to market complexity.

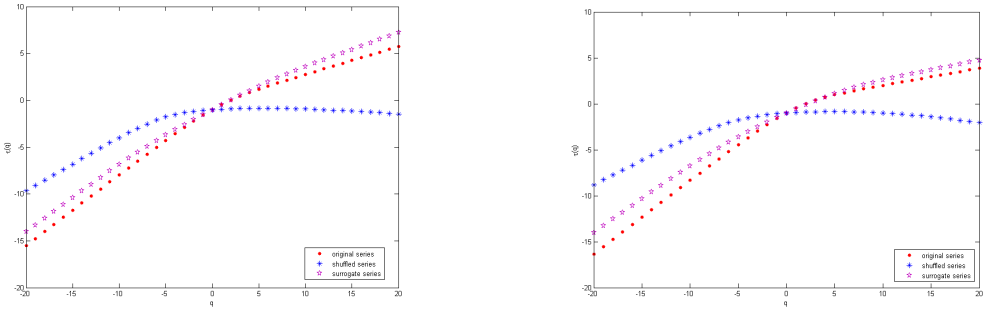

(a) Gold market (b) Silver market

Figure 7: Scaling exponents $\tau(q)$ versus order q for original, shuffled, and surrogate series. The curvature of $\tau(q)$ quantifies the degree of multifractality, with silver showing stronger nonlinearity than gold.

3.5 Multifractal Spectrum and Risk Assessment

The singularity spectrum $f(\alpha)$, derived via Legendre transform of $\tau(q)$, quantifies market risk through its width $\Delta\alpha = \alpha_{\max} - \alpha_{\min}$. Figures 8a and 8b present $f(\alpha)$ for both metals, with corresponding $\Delta\alpha$ values in Table 6.

Silver exhibits wider spectra ($\Delta\alpha = 0.6160$) than gold ($\Delta\alpha = 0.4625$), confirming higher market risk. The narrowing of spectra after phase randomization indicates that extreme events (non-Gaussian tails) contribute significantly to multifractality, particularly in silver markets. The shuffled series maintain considerable spectrum width, reinforcing that temporal correlations are the primary source of multifractality.

These findings suggest that silver markets offer higher profit potential but with elevated risk, making them more suitable for speculative investors. Gold markets, with lower multifractality and narrower spectra, provide greater stability and are more appropriate for risk-averse investors seeking safe-haven assets. The distinct risk profiles align with the fundamental characteristics of these metals: gold's role as a monetary reserve and inflation hedge versus silver's dual role as both precious metal and industrial commodity.

Table 6: Multifractality measures Δh and $\Delta\alpha$ for gold and silver markets.

	Spot Gold		Spot Silver	
Series	Δh	$\Delta\alpha$	Δh	$\Delta\alpha$
Original	0.3860	0.4625	0.5515	0.6160
Shuffled	0.3645	0.3629	0.4423	0.3947
Surrogate	0.1267	0.3178	0.1604	0.3835

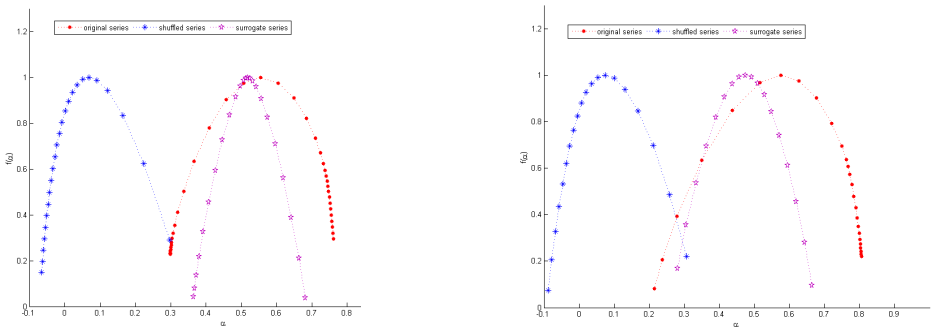

(a) Gold market (b) Silver market

Figure 8: Multifractal spectra $f(\alpha)$ for original, shuffled, and surrogate series. The width of the spectrum quantifies market risk, with silver showing consistently wider spectra than gold across all series types.

4 Conclusion and Discussion

This study enhances the Multifractal Detrended Fluctuation Analysis (MF-DFA) framework by introducing a Binary Overlapped Sliding Window-based variant (Bi-OSW-MF-DFA) and applies it to investigate the multifractal properties and risk profiles of spot gold and silver markets. Our principal findings are summarized as follows:

1. **Methodological Innovation:** We propose the Bi-OSW-MF-DFA method, which improves upon conventional MF-DFA by mitigating boundary discontinuities and enhancing statistical efficiency. The overlapping window design ensures smoother transitions between segments, while binary partitioning maintains data coverage. Empirical comparisons demonstrate that Bi-OSW-MF-DFA yields more concentrated and stable estimates of the generalized Hurst exponent $h(q)$, with reduced multifractal width measures ($\Delta h_g^* = 0.3860$ vs. $\Delta h_g = 0.5965$ for gold; $\Delta h_s^* = 0.5515$ vs. $\Delta h_s = 0.8501$ for silver).

2. **Multifractal Market Characteristics:** Both gold and silver markets exhibit clear multifractal scaling, as evidenced by crossover points in fluctuation functions $F_q(s)$ and the nonlinear dependence of $h(q)$ on q. The degree of multifractality is more pronounced in silver ($\Delta h_s^* = 0.5515$) than in gold ($\Delta h_g^* = 0.3860$), indicating higher market complexity and stronger persistence of extreme fluctuations in silver.

3. **Sources of Multifractality:** Through shuffling and phase randomization experiments, we disentangle the contributions of temporal correlations and distributional properties to multifractality. Shuffling—which destroys correlations—produces a sharp reduction in $h(q)$, confirming that long-range dependence is the primary driver of multifractality in both markets. Phase randomization—which Gaussianizes the distribution—reveals an additional, though smaller, contribution from fat-tailed return distributions, particularly in silver.

4. **Risk Implications:** The multifractal spectrum width $\Delta\alpha$ is significantly wider for silver (0.6160) than for gold (0.4625), implying greater heterogeneity in price fluctuations and higher inherent risk in the silver market. Wider spectra correspond to more pronounced price oscillations and higher potential returns, making silver attractive for speculative strategies. Conversely, gold's narrower spectrum reflects more stable price dynamics, reinforcing its role as a safe-haven asset for risk-averse investors.

The empirical results align with market observations: silver's lower trading volume and higher speculative participation amplify its price volatility, while gold's status as a reserve asset lends it greater stability. Although precious metals markets are less mature than equity or bond markets, their complex multifractal structure offers rich information for risk management and portfolio construction.

Future research could extend the Bi-OSW-MF-DFA framework to other asset classes, examine intraday high-frequency data, or incorporate macroeconomic variables to better understand the drivers of multifractality. Additionally, integrating machine-learning techniques with multifractal features may improve forecasting accuracy for extreme market movements. Investigating the impact of major economic events (such as the 2008 financial crisis or COVID-19 pandemic) on the multifractal properties of precious metals could provide further insights into market resilience and contagion effects.

In summary, this study provides both a methodological advance in multifractal analysis and actionable insights for investors and risk managers in precious metals markets. The proposed Bi-OSW-MF-DFA method offers a more reliable tool for characterizing market complexity, while the comparative analysis of gold and silver highlights distinct risk-return profiles that can inform investment and hedging strategies.

Acknowledgments

The authors sincerely thank the referees and the Editor for their valuable comments and suggestions, which have greatly improved this paper. We also acknowledge the use of DeepSeek for assistance in improving the English grammar and language clarity.

Funding

This work was supported by the National Natural Science Foundation of China (No. 61304181), BNBU Research Grants (R201912 and R202010), Curriculum Development and Teaching Enhancement (UICR0400046-21CTL), Guangdong Provincial/Zhuhai Key Laboratory of Interdisciplinary Research and Application for Data Science, BNBU (2022B1212010006), and Guangdong Higher Education Upgrading Plan (2021-2025) (UICR0400001-22).

Disclosure Statement

No potential conflict of interest was reported by the author(s).
Note: The review process for this article was handled independently by the Editor Dr. Yasser Abdel Sattar.

Data Availability Statement

The datasets analyzed during this study were obtained from the JIJIN silver and gold analysis software. The analytical methods and results are fully detailed in this manuscript, and a preprint version of this paper is available on arXiv at `https://arxiv.org/abs/2006.15214`.

References

[1] Yuan Y., and Zhuang X.T. (2008). Multifractal description of stock price index fluctuation using a quadratic fitting. *Physica A* 387: 511-518.

[2] Mali P., and Mukhopadhyay A. (2014). Multifractal characterization of gold market: A multifractal detrended fluctuation analysis. *Physica A* 413: 361-372.

[3] Hasan R., and Salim M.S. (2015). Multifractal analysis of Asian markets during 2007-2008 financial crisis. *Physica A* 419: 746-761.

[4] Ribeiro M.B., and Miguelote A.Y. (1998). Fractals and the Distribution of Galaxies. *Brazilian Journal of Physics*: 132-134.

[5] Li J., and Chen Y. (2001). Rescaled range (R/S) analysis on seismic activity parameters. *Acta Seismologica Sinica* 14(2): 148-155.

[6] Lee K.E., and Lee J.W. (2005). Multifractality of the KOSPI in Korean stock market. *Journal of the Korean Physical Society* 46: 726-729.

[7] Chen Z., Ivanov P.C., Hu K., and Stanley H.E. (2002). Effect of nonstationarities on detrended fluctuation analysis. *Physical Review E* 65(4): 041107.

[8] Du G., and Ning X. (2008). Multifractal properties of Chinese stock market in Shanghai. *Physica A* 387(1): 261-269.

[9] Jiang J., Ma K., and Cai X. (2007). Non-linear characteristics and long-range correlations in Asian stock markets. *Physica A* 378: 399-407.

[10] Pavón-Domínguez P., Serrano S., Jiménez-Hornero F.J., Jiménez-Hornero J.E., Gutiérrez de Rave E., and Ariza-Villaverde A.B. (2013). Multifractal detrended fluctuation analysis of sheep livestock prices in origin. *Physica A* 392: 4466-4476.

[11] Kantelhardt J.W., Zschiegner S.A., Koscielny-Bunde E., Havlin S., Bunde A., and Stanley H.E. (2002). Multifractal detrended fluctuation analysis of nonstationary time series. *Physica A* 316: 87-114.

[12] Zunino L., Tabak B.M., Figliola A., Perez D.G., Garavaglia M., and Rosso O.A. (2008). A multifractal approach for stock market inefficiency. *Physica A* 387: 6558-6566.

[13] Norouzzadeh P., and Jafari G.R. (2005). Application of multifractal measures to Tehran price index. *Physica A* 356: 609-627.

[14] Matia K., Ashkenazy Y., and Stanley H.E. (2003). Multifractal properties of price fluctuations of stock and commodities. *Europhysics Letters* 61(3): 422-428.

[15] Suarez-Garcia P., and Gomez-Ullate D. (2014). Multifractality and long memory of a financial index. *Physica A* 394: 226-234.

[16] Bashan A., Bartsch R., Kantelhardt J.W., and Havlin S. (2008). Comparison of detrending methods for fluctuation analysis. *Physica A* 387: 5080-5090.

[17] Yuan Y., Zhuang X.T., and Jin X. (2009). Measuring multifractality of stock price fluctuation using multifractal detrended fluctuation analysis. *Physica A* 388(11): 2189-2197.

[18] Zhou W.X. (2009). The components of empirical multifractality in financial returns. *Europhysics Letters* 88: 28004.

[19] Chen H.G., and Zhou D.Q. (2010). Multifractal spectrum analysis of crude oil futures prices volatility in NYMEX. In: *Management and Service Science (MASS)*: 1-4.

[20] Wang F., Liao G.P., Li J.H., Li X.C., and Zhou T.J. (2013). Multifractal detrended fluctuation analysis for clustering structures of electricity price periods. *Physica A* 392: 5723-5734.

[21] Aslanidis N., and Fountas S. (2014). Is real GDP stationary? Evidence from a panel unit root test with cross-sectional dependence and historical data. *Empirical Economics* 46: 101-108.